Original Article

Circ_0000228 Promotes Cervical Cancer Progression via Regulating miR-337-3p/TGFBR1 Axis

Yongqian Xu, Ph.D., Xiaona Dong, B.Sc., Baoli Ma, B.Sc., Pingping Mu, B.Sc., Xiang Kong, B.Sc.*, Dongmei Li, B.Sc.*

Department of Gynecology and Obstetrics, Shengli Oilfield Central Hospital, Dongying, Shandong, China.

**Corresponding Address: Department of Gynecology and Obstetrics, Shengli Oilfield Central Hospital, Dongying, Shandong, China
Emails: drkongxiang@21cn.com, jibimibai18507@163.com*

Abstract

Objective: This study aims to investigate the biological function of circular RNA (circRNA) circ_0000228 in the cervical cancer (CC).

Materials and Methods: In this experimental study, the GSE113696 dataset was downloaded from the Gene Expression Omnibus (GEO). GEO2R was employed to obtain differentially expressed circRNA between CC tissues and matched paracancerous tissues. Quantitative real-time polymerase chain reaction (qRT-PCR) and Western blot were employed to detect circ_0000228, microRNA-337-3p (miR-337-3p) and transforming growth factor, beta receptor I (TGFBR1) expression levels in the CC tissues and cells. Following gain-of-function and loss-of-function models establishment, CCK-8 and BrdU tests were conducted to examine cell proliferation. Transwell experiment was executed to examine CC cells migration and invasion. A lung metastasis model was utilized to determine the ability of circ_0000228 on the lung metastasis. Bioinformatics analysis, dual-luciferase reporter experiment and RNA immunoprecipitation (RIP) assay were applied to verify the targeting relationship among miR-337-3p, circ_0000228, and TGFBR1.

Results: Circ_0000228 expression in the CC tissues and cells was up-modulated. Circ_0000228 overexpression markedly enhanced cell proliferation, migration, and invasion, while knocking down circ_0000228 remarkably repressed cell proliferation, migration, and invasion. MiR-337-3p could be adsorbed by circ_0000228. TGFBR1 was identified as a target gene of miR-337-3p that indirectly and positively modulated by circ_0000228 in the CC cells.

Conclusion: Circ_0000228 up-modulates TGFBR1 by targeting miR-337-3p to enhance CC cell proliferation, migration and invasion. Also, Circ_0000228 is a promising therapeutic target for the CC.

Keywords: Cervical Cancer, miR-337-3p, TGFBR1

Introduction

Cervical cancer (CC), a common malignancy, seriously threatens women's health (1) and also, surgery, chemotherapy and radiation therapy are considered as approaches for CC treatment (2). Unfortunately, the majority of patients have reached an advanced stage by the time of diagnosis, resulting in losing the opportunity for radical surgery (3). It is of great clinical value to decipher the CC pathogenesis to reach target therapy, particularly in the advanced stage.

Circular RNAs (circRNAs) as a member of endogenous non-coding RNAs, are closed-loop RNA molecules that are formed by reverse splicing. There are not 5'-end cap and 3'-end poly A tail in their structure. Also, they can be stably present in the diverse eukaryotic cells (4). Previously, circRNAs were considered as a "noise" of gene transcription (5, 6). However, recently, their biological function has been revealed (5, 7). Some studies have shown, abnormal expression of circRNAs in the human malignancies with unfavorable prognosis (8-15). For instance, in gastric cancer, circ-DONSON promotes the proliferation, migration, and invasion of cancer cells, and impedes apoptosis (13). In CC, circ_0000515 and circ_0007534 facilitate proliferation, migration and invasion of CC cells and repress apoptosis (14, 15).

Also, circ_0000228 is generated from zinc finger E-box binding homeobox 1 (ZEB1) transcription. ZEB1 has been reported to be up-regulated in the CC and acts as an oncogene (16). Nonetheless, the biological function and mechanism of circ_0000228 in CC is undefined.

MicroRNA (miRNA, miR)-337-3p is down-modulated in the CC cells and suppresses proliferation, migration and invasion of these cells and induces apoptosis (17, 18). Also, TGFBR1 is reported to be overexpressed in the CC, and can enhance CC cell malignancy (19). Bioinformatics analysis predicts that miR-337-3p targets the 3′UTR of transforming growth factor, beta receptor I (TGFBR1). Moreover, circ_0000228 is predicted to be a potential molecular sponge for miR-337-3p. In this study, we probe function and mechanism of circ_0000228, miR-337-3p and TGFBR1 in the CC progression. We aim to offer clues to improve clinical diagnosis and therapy of CC.

Materials and Methods

Specimens collection

The work was approved by the Ethics Committee of Shengli Oilfield Central Hospital (2018-06). Totally, 57 CC specimens and corresponding cervical paracancerous specimens were surgically obtained of patients who

referred to the Shengli Oilfield Central Hospital. The patients with pathologically diagnosed CC who are willing to provide written informed consents participated in this study. The specimens were stored in the liquid nitrogen. All subjects did not undergo radiotherapy, chemotherapy or other anti-cancer treatments before surgery. All subjects signed an informed consent form before the surgery and tissue collection.

Cell culture

Human cervical epithelial cells (HUCECs) and CC cell lines (SiHa, HeLa, CaSKi, and C33A) were purchased from the Cell Center of Chinese Academy of Sciences (Shanghai, China). All cell lines were cultured in Dulbecco's Modified Eagle Medium (DMEM) medium (Cat No. 11965-092, Invitrogen, Carlsbad, CA, USA) containing 10% fetal bovine serum (FBS, Cat No. 10270098, Gibco, Grand Island, NY, USA)+100 U/mL penicillin+100 µg/mL streptomycin (Cat No. 15140122, Hyclone, Logan, UT, USA). Then, all were incubated at 37°C, 5% CO_2, 95% humidity

Cell transfection

Small interfering RNA (siRNA) negative control (si-NC), siRNA against circ_0000228-1 (si-circ_0000228-1), siRNA against circ_0000228-2 (si-circ_0000228-2), pcDNA empty vector (NC), pcDNA-*circ_0000228* (*circ_0000228*), mimics negative control (mimics NC), miRNA inhibitors negative control (inhibitors NC), *miR-337-3p* mimics, and *miR-337-3p* inhibitors were available from GenePharma Co., Ltd (Cat No. MIN0000578, Shanghai, China).

HeLa and C33A cells were planted in 6-well plates (3×10^5 cells/mL) (Cat No. 353046, BD Biosciences, Bedford, MA, USA) and cultured at 37°C with 5% CO_2 for 24 hours. Then, cells were transfected using Lipofectamine® 3000 (Cat No. L3000015, Invitrogen, Carlsbad, CA, USA) according to the manufacture's instruction. Quantitative real-time polymerase chain reaction (qRT-PCR) was performed to detect the transfection efficiency.

Quantitative real-time polymerase chain reaction

Using TRIzol reagent (Cat No. 15596-018, Invitrogen, Carlsbad, CA, USA), total RNA was extracted from CC tissues and cells. Then, the PrimeScript™ RT Reagent kit (Cat No. RR037A, Takara Biotechnology Co., Ltd., Dalian, China) was utilized to reverse transcribe total RNA into cDNA. Next, qRT-PCR was implemented using SYBR®Premix-Ex-Taq™ (Cat No. 368706, Takara, Dalian, China) on the ABI7500 FAST Real-Time PCR system (Thermo Fisher Scientific, Waltham, MA, USA). *GAPDH* was regarded as an internal reference to quantify *circ_0000228* and *TGFBR1* mRNA expression levels, and *U6* was considered as an internal reference to detect *miR-337-3p* expression. *Circ_0000228, miR-337-3p*, and *TGFBR1* mRNA relative expression was calculated using the $2^{-\Delta\Delta CT}$ method. A PARIS™ Kit (Cat No. AM1556,

Ambion, Austin, TX, USA) was employed for subcellular fractionation. After the cytoplasmic RNA and nuclear RNA were isolated respectively, qRT-PCR was executed to evaluate *circ_0000228* expression in cytoplasm and nuclei. The primer sequences used for qRT-PCR were as follows:

circ_0000228-

F: 5′-GAGGTGTGGGGTGTGAGAAC-3′
R: 5′- GCAGACAGTAGCCAAATCACA-3′

miR-337-3p-

F: 5′- CUCCUAUAUGAUGCCUUUCUUC-3′
R: 5′-GAAGAAAGGCAUCAUCUAGGAG-3′

TGFBR1-

F: 5′-CACAGAGTGGGAACAAAAAGGT-3′
R: 5′- CCAATGGAACATCGTCGAGCA-3′

U6-

F: 5′-GCCGTTGCAGCACATATACAATAAT-3′
R: 5′-CGCTACGTTAATGCTCGTGTCAT-3′

GAPDH-

F: 5′-AGAAGGCTGGGGCTCATTTG-3′
R: 5′-AGGGGCCATCCACAGTCTTC-3′

Colorimetric measurement of cell proliferation

After trypsinization, both cells, HeLa and C33A, were harvested. Then the cells were inoculated in a 96-well plate (2×10^3 cells/well) and incubated. After 24 hours, 10 µL of cell counting kit8 (CCK-8) solution (Cat No. HY-K 0301, MedChemExpress, Monmouth Junction, NJ, USA) was supplemented to each well and then the cell culture was continued for 1 hour. The absorbance (OD_{450nm} value) of each well was recorded using a Bio-Tek Synergy HT Microplate Reader (Bio-Tek Instruments, Winooski, VT, USA). Thereafter, with the same method, the absorbance of the cells was measured 48 hours and 72 hours later, respectively.

BrdU experiment

Cell proliferation was also assessed with the BrdU Cell Proliferation Assay kit (Cat No. 6813, Beyotime, Shanghai, China). The single-cell suspension was prepared with HeLa and C33A cells, and the cells were inoculated into 96-well plates (1×10^4 per well). Subsequently, 20 µl BrdU solution was added to each well and incubated for 24 hours. Subsequently, the culture medium was discarded and the cells were washed with PBS. Cells were fixed with 4% paraformaldehyde for 30 min at room temperature and washed again with PBS. Cells were incubated with anti-BrdU (Cat No. ab6326, Abcam, Shanghai, China) for 1 hour at room temperature. Then, cell nuclei were counterstained using Hoechst staining solution (Beyotime, Shanghai, China) at room temperature for 30 minutes. After PBS washing, the cells were incubated with pre-diluted detection antibody for 1 hour. Thereafter, the cells

were stained with Hoechst staining solution. The total number of cells and the number of BrdU-positive cells in 10 high magnification fields were counted randomly under the microscope, and the percentage of BrdU-positive cells was calculated.

Transswell experiment

In the migration experiments, HeLa and C33A cells were resuspended in the serum-free medium, and the cell density was modulated (2×10^5 cells / mL), and then 100 µL of the cell suspension was supplemented to the upper compartment of the Transwell system (Cat No. 3422, Corning, Corning, NY, USA). Then, 500 µl DMEM medium containing 10% FBS was supplemented to the lower compartment of the Transwell chamber. 24 hours' incubation at room temperature, the upper compartment cells that did not migrate were gently wiped off with cotton swabs, and the attached cells on the lower surface of the membrane were fixed with 4% paraformaldehyde (Cat No. J61899, Alfa Aesar, averhill, MA, USA). After that, the cells were stained with 0.1% crystal violet (Cat No. C0121, Beyotime, Shanghai, China) for 10 minutes. After the membranes were washed, five randomly selected microscopic fields per membrane was selected and the numbers of stained cells were counted. To perform the cell invasion assay, the Transwell inserts were pre-covered with 50 ml of the Matrigel matrix. DMEM medium containing 10% FBS was placed in the lower chamber as a chemoattractant. Twenty-four hours later, 0.1% crystal violet was used to stain the cells that had invaded through the membranes. Then, the cells were observed by a microscope.

Dual-luciferase reporter assay system

The dual-luciferase reporter assay system (Cat No. 11752250, Promega, Madison, WI, USA) was used in this experiment. HeLa and C33A cells were trypsinized, counted, and planted in a 24-well plate (1×10^4 cells/well), and cultured for 24 hours. When cell confluence reached 80-90%, the transfection was performed with Lipofectamine® 3000 (Invitrogen, Carlsbad, CA, USA). Wild-type *circ_0000228* (WT circ_0000228), wild-type *TGFBR1* (WT *TGFBR1*), mutant-type *circ_0000228* (MUT circ_0000228) and mutant-type *TGFBR1* (MUT *TGFBR1*) reporter vectors were co-transfected with mimics NC, *miR-337-3p* mimics and *miR-337-3p* inhibitors, respectively. After the cells were cultured for 48 hours, the cells were collected, lysed with lysis buffer, and the supernatant was collected. Following that, the luciferase substrate was added and the luciferase activity was examined by the luminometer (Glomax 96 Microplate Luminometer, Promega, Madison, WI, USA). Firefly luciferase activity was normalized to the Renilla luciferase activity.

RNA immunoprecipitation assay

Using Magna RIP™ RNA‑Binding Protein Immunoprecipitation Ki (Cat No. 17-700, Millipore, Billerica, MA, USA), the interaction between circ_0000228 and miR-337-3p was evaluated. Both cells, HeLa and C33A, were lysed in the RIP lysis buffer, and 100 µL of cell lysates were incubated with magnetic beads coupling with anti-Argonaute2 (Ago2) antibody or negative control IgG in the RIP buffer. Then the specimens were incubated with Proteinase K (Cat No. 25530-031, Invitrogen, Carlsbad, CA, USA) to remove proteins and then RNA precipitation was obtained. The purified RNA was subjected to qRT-PCR analysis.

Western blot

48 hours after transfection, HeLa and C33A cells were lysed with RIPA lysis buffer (Cat# P0013B, Beyotime Biotechnology, Shanghai, China) containing protease inhibitors (Cat No. 11836170001, Roche Applied Science, Penzberg, Germany), and the supernatants were collected after high-speed centrifugation, and protein concentrations were determined by a BCA kit (Cat No. P0012S, Beyotime, Shanghai, China). The supernatant was mixed with loading buffer, and then heated in a water bath at 100°C for 10 minutes to denature the protein. Next, the total proteins were separated using sodium dodecyl sulfate-polyacrylamide gel electrophoresis (SDS-PAGE) and transferred to polyvinylidene difluoride (PVDF) membranes by electrotransfer. The membranes were then incubated with the specific primary antibodies overnight at 4°C. After rinsing with Tween-20 (TBST, Cat No. AAJ77500K8, Fisher Scientific, Houston, TX, USA), the membranes were then incubated with corresponding secondary antibodies for 2 hours at room temperature. The protein bands were visualized by electrochemiluminescence automatic chemiluminescence imaging analysis system (Tanon 5500, Tanon Science & Technology, Shanghai, China), and β-actin was regarded as an internal reference. The antibodies used in this work were available from Abcam (Shanghai, China), including primary antibodies: anti-TGFBR1 antibody (ab31013, 1:1000), anti-β-actin antibody (ab179467, 1:1000), and a secondary antibody (ab205718, 1:2000).

Lung metastasis experiment

The protocol of animal experiments was approved by the Institutional Animal Care and Use Committee of Shengli Oilfield Central Hospital. 12 male BALB/C nude mice (4 weeks old, Vital River Laboratory Animal Technology, Beijing, China) were utilized for lung metastasis experiments, to evaluate the metastatic ability of CC cells *in vivo*. Mice were housed under standard housing conditions (23°C, 40% humidity, 12 hours/12 hours light-dark cycle, food and water were available). Then, HeLa cells (1×10^7 cells/per mouse) transfected with *circ_0000228* overexpression or empty vector plasmid were injected into the tail veins of nude mice (6 mice/per group). After 4 weeks, the mice were euthanized and the lung tissues were obtained. Next, hematoxylin/eosin staining was performed to show the metastatic nodules.

Statistical analysis

All data were analyzed using GraphPad Prism 8 (GraphPad Software, La Jolla, CA, USA). Shapiro-Wilk

(SW) test was used to analyze the normal distribution of the data. All the measurement data were expressed as "mean ± standard deviation" (mean ± SD). Also, t test was adopted for comparison between two groups, and one-way ANOVA was used for comparison of the means among multiple groups. For skewed distributed data, the Wilcoxon signed-rank test was used. Counting data were expressed in contingency tables, and χ2 test was utilized to analyze differences between the two groups. Statistical significance was indicated by P<0.05.

Results

Circ_0000228 expression was up-modulated in cervical cancer

Detecting circRNA expression profile in the CC tissues, we observed that 122 circRNAs were down-modulated (P<0.05), while 34 circRNAs (including circ_0000228) were up-modulated (Fig.1A, B, P<0.05). Consistently, qRT-PCR indicated that circ_0000228 was up-modulated in the CC tissues (n=57) in comparison with the matched non-cancerous tissues (Fig.1C, P<0.001). Analyzing relationship between circ_0000228 expression in the CC tissues and clinical parameters, we observed that high circ_0000228 expression in the CC tissues was linked to lymph node metastasis and low differentiation of tumor tissues (Fig.1D, Table 1, P<0.05). Additionally, circ_0000228 expression was up-modulated in all of the 4 CC cell lines (SiHa, HeLa, CaSKi, C33A) relative to normal cervical epithelial cell line HUCEC cell (Fig.1E, P<0.01).

Circ_0000228 enhanced the proliferation, migration and invasion of cervical cancer cells

To examine the biological role of *circ_0000228* in the CC, HeLa cells were transfected with *circ_0000228* overexpression plasmid. Also, C33A cells were transfected with si-circ_0000228-1 and si-circ_0000228-2 (Fig.2A). CCK-8 colorimetric assay unveiled that *circ_0000228* overexpression facilitates the proliferation of HeLa cells (P<0.001), while knock down *circ_0000228* restrained C33A cell proliferation (Fig.2B, P<0.001). The data of BrdU experiments manifested, that the number of BrdU-positive cells was higher in the *circ_0000228* overexpression group in comparison with the control group (P<0.001). The BrdU-positive cells number was lower in the si-circ_0000228-1 and si-circ_0000228-2 groups (Fig.2C, P<0.001). And, Transwell experiment was executed to examine the effects of *circ_0000228* on the CC cell migration and invasion. The results demonstrated that *circ_0000228* overexpression facilitates migration of HeLa cell and invasion (P<0.001), while *circ_0000228* knockdown restrained C33A cells migration and invasion (Fig.2D, P<0.001). Finally, we used a lung metastasis model, *in vivo* model, to investigate the role of *circ_0000228* in the CC cells metastasis regulation. The results indicated that *circ_0000228* overexpression promoted lung metastasis *in vivo* (Fig.S1, See Supplementrary Online Information at www.celljournal.org, P<0.001).
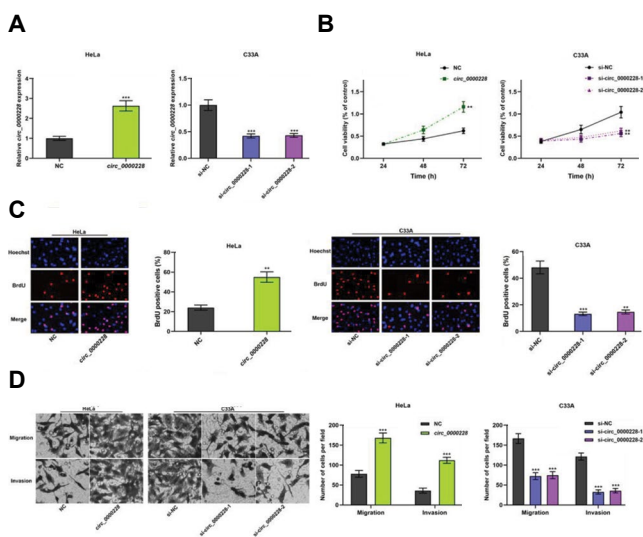
Table 1: Correlation between clinicopathological features and expression of circ_0000228 in the CC tissues

Pathological parameters	Numbers (n=57)	Circ_0000228 expression		χ2	P value
		High (n=28)	Low (n=29)		
Age (Y)				0.4220	0.5159
<45	33	15	18		
≥45	24	13	11		
Tumor size (cm)				1.4164	0.2340
<4	29	12	17		
>4	28	16	12		
FIGO stage				0.8884	0.3459
I	26	11	15		
II	31	17	14		
Lymph node metastasis				4.1352	0.0420*
No	24	8	16		
Yes	33	20	13		
Degree of differentiation				9.4270	0.0021*
Poor, moderate	31	21	10		
Well	26	7	19		

CC; Cervical cancer, FIGO; International federation of gynecology and obstetrics, and *; P<0.05.
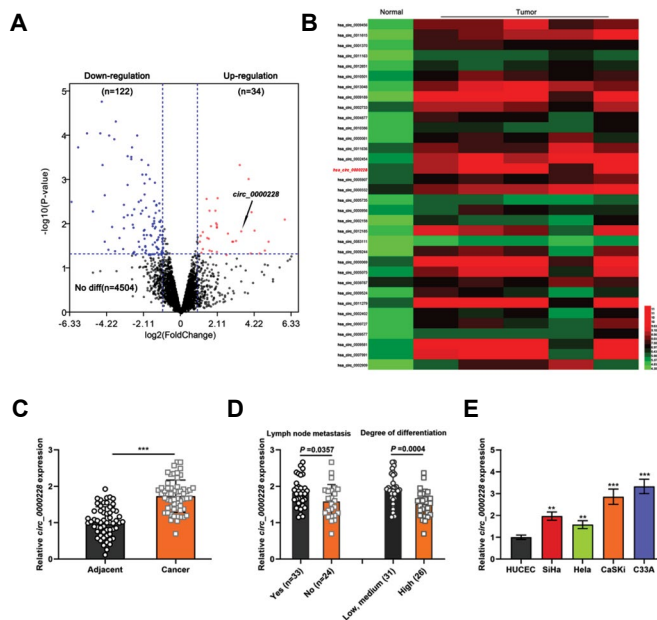
Fig.1: The expression characteristics of circ_0000228 in CC. **A, B.** Variations in the expression of circRNAs in the CC tissues were examined by analyzing dataset GSE113696. **C.** qRT-PCR was executed to examine *circ_0000228* expression in the 57 cases of CC tissues and matched paracancerous tissues. **D.** qRT-PCR was implemented to examine *circ_0000228* expression in the CC tissues of the patients with lymph node metastasis and without lymph node metastasis, different differentiation status, respectively. **E.** *Circ_0000228* expression in the HUCECs and CC cell lines (SiHa, HeLa, CaSKi and C33A) was measured by qRT-PCR. CC; cervical cancer, qRT-PCR; Quantitative real-time polymerase chain reaction, HUCECs; Human cervical epithelial cells, **; P<0.01, and ***; P<0.001.

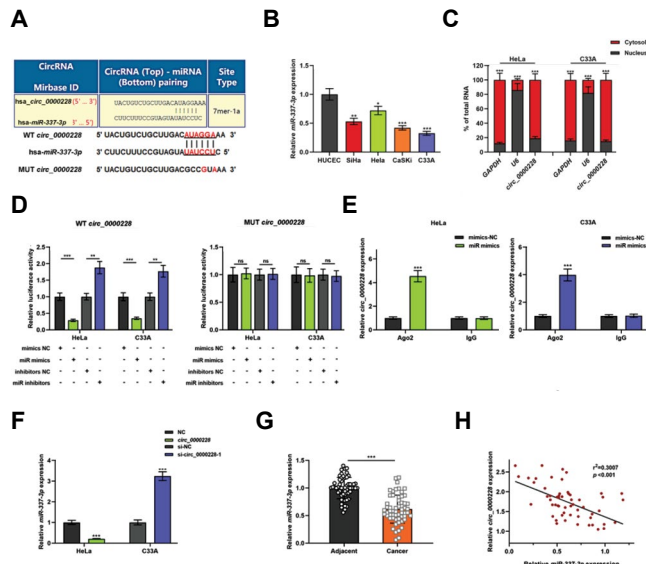the CircInteractome database (https://circinteractome. nia.nih.gov/) was searched. *miR-337-3p* was selected as a one of the predicted target miRNAs (Fig.3A, P<0.001). Subsequently, *miR-337-3p* expression in the CC cell lines was examined by qRT-PCR. *miR-337-3p* expression was demonstrated to be diminished in the CC cell lines (Fig.3B, P<0.05). Nucleocytoplasmic separation assay showed that *circ_0000228* was expressed in the CC cells cytoplasm (Fig.3C, P<0.001). Dual-luciferase reporter experiment showed that *miR-337-3p* overexpression repressed the luciferase activity of WT *circ_0000228*, while *miR-337-3p* inhibition enhanced the luciferase activity of WT *circ_0000228* (Fig.3D, P<0.001). However, neither miR-337-3p mimic nor miR-337-3p inhibitor affected the luciferase activity of MUT *circ_0000228* (Fig.3D). Next, the results of RIP experiments showed that *circ_0000228* and *miR-337-3p* were enriched in the Ago2-containing microribonucleoproteins relative to IgG group, suggesting a direct interaction between *circ_0000228* and *miR-337-3p* (Fig.3E, P<0.001). Moreover, *circ_0000228* overexpression suppressed *miR-337-3p* expression in the HeLa cells; while *circ_0000228* knock down *circ_0000228* increased *miR-337-3p* expression in the C33A cells (Fig.3F, P<0.001). Also, *miR-337-3p* was unveiled to be down-modulated in the CC tissues by qRT-PCR (Fig.3G, P<0.001). Pearson's correlation analysis indicated that *circ_0000228* was negatively correlated with *miR-337-3p* expression in the CC tissues (Fig.3H, P<0.001).

Fig.2: Regulatory role of *circ_0000228* in the CC cells phenotype. **A.** HeLa and C33A cells were transfected with *circ_0000228* overexpression plasmid and *circ_0000228* siRNAs, respectively, and also, the transfection efficiency was examined by qRT-PCR. **B, C.** The effects of *circ_0000228* overexpression or knockdown on the proliferation of HeLa and C33A cells were detected using CCK-8 colorimetric assay and BrdU experiment. **D.** Transwell experiments were used to examine the effects of *circ_0000228* overexpression and knockdown on the migration and invasion of HeLa and C33A cells. CC; Cervical cancer, qRT-PCR; Quantitative real-time polymerase chain reaction, **; P<0.01, and ***; P<0.001.

Circ_0000228 directly targeted *miR-337-3p*

To probe the downstream targets of *circ_0000228*,

Fig.3: *Circ_0000228* directly targeted *miR-337-3p*. **A.** Bioinformatics analysis projected the binding site between *circ_0000228* and *miR-337-3p*. **B.** *MiR-337-3p* expression in the CC cell lines and HUCECs was examined by qRT-PCR. **C.** Nucleocytoplasmic separation experiment was conducted to verify the localization of *circ_0000228* in the CC cells. **D.** Dual-luciferase reporter gene experiment was implemented to validate the bioinformatics predicted binding site. **E.** RIP assays were utilized to prove the interaction between *circ_0000228* with *miR-337-3p*. **F.** The effect of *circ_0000228* overexpression and knockdown on the *miR-337-3p* expression in the CC cells was detected by qRT-PCR. **G.** *MiR-337-3p* expression in the 57 CC tissues and 57 paracancerous tissues was examined by qRT-PCR. **H.** Pearson's correlation analysis assessed the correlation between *miR-337-3p* expression and *circ_0000228* expression in the CC tissues. CC; Cervical cancer, qRT-PCR; Quantitative real-time polymerase chain reaction, RIP; RNA immunoprecipitation, *; P<0.05, **; P<0.01, and ***; P<0.001.

Circ_0000228 regulated the proliferation, migration and invasion of cervical cancer cells by adsorbing *miR-337-3p*

Subsequently, *circ_0000228* overexpression plasmid and *miR-337-3p* mimics were co-transfected into the HeLa cells. Also, si-circ_0000228-1 and *miR-337-3p* inhibitors were co-transfected into the C33A cells (Fig.4A). CCK-8 colorimetric assay, BrdU experiments and Transwell experiments showed that *circ_0000228* overexpression facilitated CC cell proliferation, migration and invasion (P<0.05), while transfection with *miR-337-3p* mimics attenuated these effects (P<0.05). On the other hand, knocking down *circ_0000228* repressed cell proliferation, migration, and invasion (P<0.05), while transfection of *miR-337-3p* inhibitors partially reversed these effects (Fig.4B-D, P<0.05).
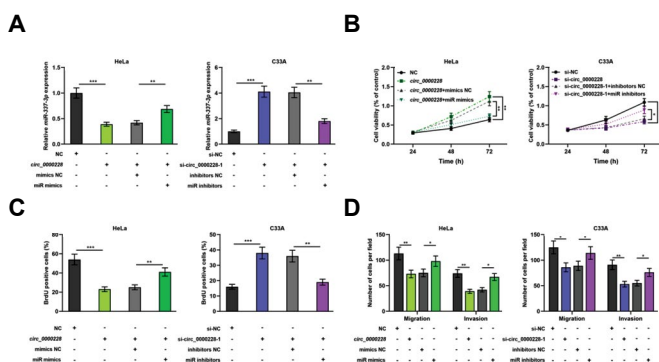

Fig.4: The effect of *circ_0000228/miR-337-3p* axis on the proliferation, migration and invasion of the CC cells. **A.** HeLa cells were co-transfected with *circ_0000228* overexpression plasmid and *miR-337-3p* mimics, and C33A cells were co-transfected with si-circ_0000228-1 and *miR-337-3p* inhibitors, and then the transfection efficiency was determined by qRT-PCR. **B, C.** CCK-8 colorimetric assay and BrdU experiments were used to examine the effects of *circ_0000228* and *miR-337-3p* on CC cell proliferation. **D.** Transwell test was applied to examine the effects of *circ_0000228* and *miR-337-3p* on the CC cell migration and invasion. CC; Cervical cancer, qRT-PCR; Quantitative real-time polymerase chain reaction, *; P<0.05, **; P<0.01, ***; P<0.001.

Circ_0000228 targeted *miR-337-3p* to up-modulate *TGFBR1* expression

The TargetScan database (http://www.targetscan.org/vert_72/) was used to predict the downstream targets of *miR-337-3p*, and *TGFBR1* was predicted as one of the potential downstream targets of *miR-337-3p* (Fig.5A). Dual-luciferase reporter experiment showed that miR-337-3p overexpression repressed the luciferase activity of WT TGFBR1, while miR-337-3p inhibition enhanced the luciferase activity of WT TGFBR1 (Fig.5B, P<0.001). However, neither miR-337-3p mimic nor miR-337-3p inhibitor affected the luciferase activity of MUT TGFBR1 (Fig.5B).

Western blot showed that *circ_0000228* overexpression enhanced *TGFBR1* expression in the HeLa cells (P<0.001), whereas transfection of *miR-337-3p* mimics attenuated this effect (Fig.5C, P<0.001). Knocking

down *circ_0000228* impeded *TGFBR1* expression in C33A cells (P<0.001), whereas inhibition of *miR-337-3p* counteracted this effect (Fig.5C, P<0.001). By qRT-PCR, *TGFBR1* mRNA revealed overexpression in the CC tissues (Fig.5D, P<0.001). Notably, TGFBR1 mRNA expression in CC tissues was negatively correlated with miR-337-3p expression (P<0.001) and positively correlated with circ_0000228 expression (Fig.5E, F, P<0.001).
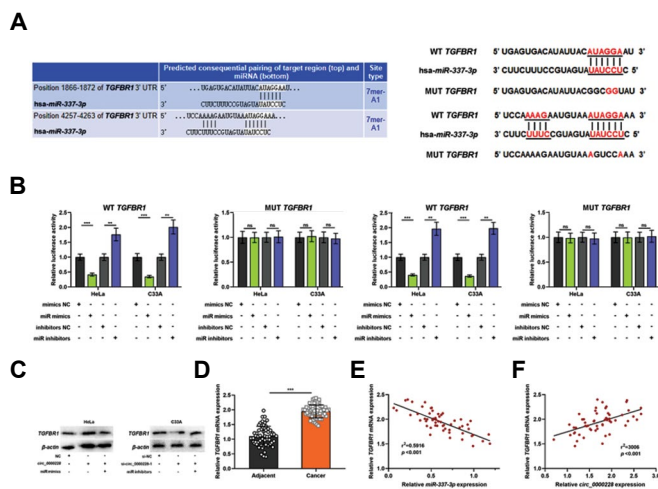
Fig.5: *Circ_0000228* up-regulated *TGFBR1* expression by sponging *miR-337-3p*. **A.** TargetScan projected the binding site between *miR-337-3p* and *TGFBR1*. **B.** Dual-luciferase reporter gene experiment was executed to prove the binding site between *miR-337-3p* and *TGFBR1* 3′UTR predicted by bioinformatics analysis. **C.** Western blot was utilized to examine the regulatory functions of circ_0000228 and miR-337-3p mimics on TGFBR1 expression. **D.** qRT-PCR was employed to examine *TGFBR1* mRNA expression in the CC tissues and paracancerous tissues. **E, F.** Pearson's correlation analysis analyzed the correlations between *TGFBR1* mRNA and *miR-337-3p/circ_0000228* expression in the CC tissues. CC; Cervical cancer, qRT-PCR; Quantitative real-time polymerase chain reaction, *; P<0.05, **; P<0.01, and ***; P<0.001.

Discussion

In this study, we observed that *circ_0000228* was up-regulated in the CC tissues and its overexpression was associated with to several adverse clinical parameters in the CC patients. Our experiments demonstrated that *circ_0000228* overexpression facilitates proliferation, migration and invasion of CC cells. We verified these findings with while knock down model of *circ_0000228*, and observed opposite effects. Several studies report that they are crucial regulators in cancer biology (20). For instance, *circ-ITCH* restrains the proliferation, migration and invasion of bladder cancer cells by sponging *miR-17/miR-224* to up-regulate PTEN expression (8). *Circ-SMARCA5* represses the development of multiple myeloma by decoying *miR-767-5p* (21). Knocking down *circ_0000285* suppresses the growth and migration of the CC cells (22). In the present work, our data indicated that *circ_0000228* is a new oncogenic factor in the CC tissues and cells.

As mentioned above, miRNAs are often negatively regulated by circRNAs via a competitive endogenous RNA mechanism (8). In this work, it was found

that *circ_0000228* directly targets *miR-337-3p* and *circ_0000228* enhances the CC cell proliferation, migration and invasion via adsorbing *miR-337-3p*. miRNAs are endogenous ncRNAs that are approximately 20 nucleotides in length that participate in the regulating diverse biological processes including epigenetic regulation, cell cycle, cell differentiation, proliferation, migration and so on (23, 24). miRNAs can function as either tumor-suppressive factors or oncogenic factors. For instance, *miR-324-3p* enhances the proliferation, migration, and invasion of colonic cancer cells, and impedes apoptosis (25). *MiR-338-3p* restrains CC progression by targeting *MACC1* to regulate the MAPK signaling pathway (26). *MiR-1284* represses the growth and metastasis of CC cells by targeting *HMGB1* and increases the sensitivity of CC cells to cisplatin (27). It is reported that *miR-337-3p* was a tumor suppressor in the CC cells and tissues (17, 18). Here, we reported that *miR-337-3p* counteracts with cancer-promoting effects of *circ_0000228* in CC cells and tissues, which also validated the anti-cancer effects of *miR-337-3p*. Moreover, we demonstrated that *miR-337-3p* can be adsorbed by circ_0000228, which is a reasonable explanation for the aberrant expression of *miR-337-3p* in the CC cells and tissues.

Usually, miRNAs exert their biological functions through binding to the 3′UTR of mRNAs target to induce translational repression or degradation of mRNAs (23). In this work, we found that *miR-337-3p* directly targets *TGFBR1* mRNA 3′UTR and negatively regulates *TGFBR1 mRNA* expression, and *circ_0000228* can promote *TGFBR1* expression in the CC cells. *TGFBR1* belongs to the TGF-β receptors family, which is involved in the TGF-β-mediated cell growth, differentiation and migration (28, 29). Accumulating studies have confirmed the regulatory role of *TGFBR1* in the different cancers (30-32). For instance, *TGFBR1* overexpression can enhance the proliferation, migration, invasion and the epithelial-mesenchymal transition process of gastric cancer cells (30).

In pancreatic cancer, *LINC00462* overexpression enhances the expression of *TGFBR1* and *TGFBR2*, thereby TGF-β/Smad pathway activating leads to facilitate proliferation, migration, and invasion of pancreatic cancer cells (31). In the non-small cell lung cancer (NSCLC), *miR-3607-3p* impedes tumor cell proliferation, invasion and migration by targeting *TGFBR1* (32). Also, in the CC, *TGFBR1* is reported to be a target of *let-7a*, and it mediates the activation of TGF-β/SMAD signaling in the CC cells (19). To our knowledge, this study is the first to identify *miR-337-3p* as an upstream miRNA of *TGFBR1* in the CC cells.

Conclusion

This research reveals that *circ_0000228* is highly expressed in the CC tissues and cells, and its highest expression is associated with adverse clinical parameters in the affected. Functionally and mechanistically, we confirm that *circ_0000228* enhances proliferation,

migration and invasion of CC cells via modulating the *miR-337-3p*/*TGFBR1* axis. This work may provide novel ideas for the diagnosis, therapy, and prognosis of CC patients.

Acknowledgments

Authors' Contributions

Y.X., X.D.; Contributed to conception and design. X.D., B.M., P.M.; Contributed to all experimental work, data, statistical analysis, and interpretation of data. Y.X., X.D.; Were responsible for overall supervision. Y.X., X.K., D.L.; Drafted the manuscript, which was revised by Y.X., X.D. All authors read and approved the final manuscript.

Reference

1. Bray F, Ferlay J, Soerjomataram I, Siegel RL, Torre LA, Jemal A. Global cancer statistics 2018: GLOBOCAN estimates of incidence and mortality worldwide for 36 cancers in 185 countries. CA Cancer J Clin. 2018; 68(6): 394-424.
2. Small W Jr, Bacon MA, Bajaj A, Chuang LT, Fisher BJ, Harkenrider MM, et al. Cervical cancer: a global health crisis. Cancer. 2017; 123(13): 2404-2412.
3. Ning MS, Ahobila V, Jhingran A, Stecklein SR, Frumovitz M, Schmeler KM, et al. Outcomes and patterns of relapse after definitive radiation therapy for oligometastatic cervical cancer. Gynecol Oncol. 2018; 148(1): 132-138.
4. Qu S, Yang X, Li X, Wang J, Gao Y, Shang R, et al. Circular RNA: a new star of noncoding RNAs. Cancer Lett. 2015; 365(2): 141-148.
5. Memczak S, Jens M, Elefsinioti A, Torti F, Krueger J, Rybak A, et al. Circular RNAs are a large class of animal RNAs with regulatory potency. Nature. 2013; 495(7441): 333-338.
6. Qu S, Zhong Y, Shang R, Zhang X, Song W, Kjems J, et al. The emerging landscape of circular RNA in life processes. RNA Biol. 2017; 14(8): 992-999.
7. Hansen TB, Jensen TI, Clausen BH, Bramsen JB, Finsen B, Damgaard CK, et al. Natural RNA circles function as efficient microRNA sponges. Nature. 2013; 495(7441): 384-388.
8. Yang C, Yuan W, Yang X, Li P, Wang J, Han J, et al. Circular RNA circ-ITCH inhibits bladder cancer progression by sponging miR-17/miR-224 and regulating p21, PTEN expression. Mol Cancer. 2018; 17(1): 19.
9. Du WW, Yang W, Li X, Awan FM, Yang Z, Fang L, et al. A circular RNA circ-DNMT1 enhances breast cancer progression by activating autophagy. Oncogene. 2018; 37(44): 5829-5842.
10. Guo J, Wang Z, Miao Y, Shen Y, Li M, Gong L, et al. A two-circRNA signature predicts tumour recurrence in clinical non-functioning pituitary adenoma. Oncol Rep. 2019; 41(1): 113-124.
11. Zhu X, Wang X, Wei S, Chen Y, Chen Y, Fan X, et al. hsa_circ_0013958: a circular RNA and potential novel biomarker for lung adenocarcinoma. FEBS J. 2017; 284(14): 2170-2182.
12. Zhao ZJ, Shen J. Circular RNA participates in the carcinogenesis and the malignant behavior of cancer. RNA Biol. 2017; 14(5): 514-521.
13. Ding L, Zhao Y, Dang S, Wang Y, Li X, Yu X, et al. Circular RNA circ-DONSON facilitates gastric cancer growth and invasion via NURF complex dependent activation of transcription factor SOX4. Mol Cancer. 2019; 18(1): 45.
14. Tang Q, Chen Z, Zhao L, Xu H. Circular RNA hsa_circ_0000515 acts as a miR-326 sponge to promote cervical cancer progression through up-regulation of ELK1. Aging (Albany NY). 2019; 11(22): 9982-9999.

15. Rong X, Gao W, Yang X, Guo J. Downregulation of hsa_circ_0007534 restricts the proliferation and invasion of cervical cancer through regulating miR-498/BMI-1 signaling. Life Sci. 2019; 235: 116785.

16. Chen XJ, Deng YR, Wang ZC, Wei WF, Zhou CF, Zhang YM, et al. Hypoxia-induced ZEB1 promotes cervical cancer progression via CCL8-dependent tumour-associated macrophage recruitment. Cell Death Dis. 2019; 10(7): 508.

17. Cao XM. Role of miR-337-3p and its target Rap1A in modulating proliferation, invasion, migration and apoptosis of cervical cancer cells. Cancer Biomark. 2019; 24(3): 257-67.

18. Meng QH, Li Y, Kong C, Gao XM, Jiang XJ. Circ_0000388 exerts oncogenic function in cervical cancer cells by regulating miR-337-3p/TCF12 axis. Cancer Biother Radiopharm. 20201; 36(1): 58-69.

19. Wu T, Chen X, Peng R, Liu H, Yin P, Peng H, et al. Let-7a suppresses cell proliferation via the TGF-β/SMAD signaling pathway in cervical cancer. Oncol Rep. 2016; 36(6): 3275-3282.

20. Zhang HD, Jiang LH, Sun DW, Hou JC, Ji ZL. CircRNA: a novel type of biomarker for cancer. Breast Cancer. 2018; 25(1): 1-7.

21. Liu H, Wu Y, Wang S, Jiang J, Zhang C, Jiang Y, et al. Circ-SMARCA5 suppresses progression of multiple myeloma by targeting miR-767-5p. BMC Cancer. 2019; 19(1): 937.

22. Chen RX, Liu HL, Yang LL, Kang FH, Xin LP, Huang LR, et al. Circular RNA circRNA_0000285 promotes cervical cancer development by regulating FUS. Eur Rev Med Pharmacol Sci. 2019; 23(20): 8771-8778.

23. Zhang Y, Wang Z, Gemeinhart RA. Progress in microRNA delivery. J Control Release. 2013; 172(3): 962-974.

24. Ha M, Kim VN. Regulation of microRNA biogenesis. Nat Rev Mol Cell Biol. 2014; 15(8): 509-524.

25. Yan D, Liu W, Liu Y, Luo M. LINC00261 suppresses human colon cancer progression via sponging miR-324-3p and inactivating the Wnt/β-catenin pathway. J Cell Physiol. 2019; 234(12): 22648-22656.

26. Hua FF, Liu SS, Zhu LH, Wang YH, Liang X, Ma N, et al. MiRNA-338-3p regulates cervical cancer cells proliferation by targeting MACC1 through MAPK signaling pathway. Eur Rev Med Pharmacol Sci. 2017; 21(23): 5342-5352.

27. Chen J, Li G. MiR-1284 enhances sensitivity of cervical cancer cells to cisplatin via downregulating HMGB1. Biomed Pharmacother. 2018; 107: 997-1003.

28. Morikawa M, Derynck R, Miyazono K. TGF-β and the TGF-β family: context-dependent roles in cell and tissue physiology. Cold Spring Harb Perspect Biol. 2016; 8(5): a021873.

29. Colasante A, Aiello FB, Brunetti M, di Giovine FS. Gene expression of transforming growth factor beta receptors I and II in non-small-cell lung tumors. Cytokine. 2003; 24(5): 182-189.

30. Ishimoto T, Miyake K, Nandi T, Yashiro M, Onishi N, Huang KK, et al. Activation of transforming growth factor beta 1 signaling in gastric cancer-associated fibroblasts increases their motility, via expression of rhomboid 5 homolog 2, and ability to induce invasiveness of gastric cancer cells. Gastroenterology. 2017; 153(1): 191-204. e16.

31. Zhou B, Guo W, Sun C, Zhang B, Zheng F. Linc00462 promotes pancreatic cancer invasiveness through the miR-665/TGFBR1-TGFBR2/SMAD2/3 pathway. Cell Death Dis. 2018; 9(6): 706.

32. Gao P, Wang H, Yu J, Zhang J, Yang Z, Liu M, et al. miR-3607-3p suppresses non-small cell lung cancer (NSCLC) by targeting TGFBR1 and CCNE2. PLoS Genet. 2018; 14(12): e1007790.